*Progress In Electromagnetics Research Letters, Vol. 76, 39–46, 2018*

# A Study of Designing Circular Polarization for Leaky Coaxial Cable at 900 MHz

**Qiao Guan[1, 2, *], Chongchong Chen[1, 2], and Bingxin Song[2]**

**Abstract**—Widely applied in confined areas communication, leaky coaxial cable (LCX) is used as an antenna to provide communication services for mobile devices. In order to improve the quality of mobile communication in narrow and long spaces such as subway or tunnel, the method of designing LCX with circular polarization radiation property is proposed, which consists of aperture's design, circular polarization simulation verification and coupling loss test. Firstly, the regular circumferential asymmetry apertures are designed and slotted in the outer conductor of the LCX to achieve radiating $\varphi$ component of the electric field, and the optimized size of the aperture for achieving circular polarization is obtained by the simulation results from Ansoft HFSS. Then, the circular polarization characteristics in the maximum radiation direction are obtained. Further, the relation between it and the gain of the optimized aperture is analyzed. Finally, the coupling loss is calculated for evaluating the performance of the LCX. The simulation results show that the two designed LCXs have the circumferential circular polarization range of $30 \sim 70$ deg in the maximum radiation direction at 900 MHz, and the range is twice of the conventional LCX. The coupling loss indicator also meets the requirements.

## 1. INTRODUCTION

Compared with the antenna used for a communication base station, leaky coaxial cable (LCX) can provide more uniform and stable communication quality in some application scenarios with narrow and long spaces, which is increasingly widely utilized for the subway, tunnels, and indoor communications [1–3]. Usually, when an LCX with linear polarization is applied to a public mobile communication system, the signal attenuation occurs due to the polarization mismatch between the LCX and the terminal antennas of the mobile phones. Generally, these terminal antennas are in a random polarization state which seriously affects the reliability of the public mobile communication system. Therefore, the circular polarization LCX has great potential in the field of communication, and it also plays an important role in detection sensor and RFID applications [4–6].

At present, the circular polarization degree range of the common circular polarization LCX is narrow, and the research and development of the circular polarization LCX also strongly depends on the engineering experience in the lack of theoretical analysis. In practice, a circular polarization LCX is mainly designed with a common aperture simple shape and computer simulation. Circular polarization of an LCX is hardly designed by theoretical method, due to the irregular shapes of aperture and the complicated analytical solution of the electromagnetic field [7, 8].

In order to achieve the best signal receiving state, new requirements are put forward on designing the LCX with circular polarization property. These four properties of the LCX, maximum radiation direction, circular polarization range, gain and coupling loss, are considered comprehensively in this paper. Firstly, the geometry parameters of the aperture are optimized to realize the circular polarization

*Received 3 March 2018, Accepted 4 May 2018, Scheduled 26 May 2018*

* Corresponding author: Qiao Guan (guanqiao@stu.xidian.edu.cn).

[1] School of Electronic Engineering, Xidian University, Xi'an, Shaanxi 710071, China. [2] Key Lab of High-Speed Circuit Design and EMC, Ministry of Education, Xidian University, Xi'an, Shaanxi 710071, China.

of the LCX in the maximum radiation direction at 900 MHz. Then, the relation between the degree range of the circular polarization and the maximum gain is studied, and the polarization mode is well simulated by Ansoft HFSS software. Finally, the coupling loss is discussed to evaluate the communication performance.

## 2. METHOD OF THE LCX'S CIRCULAR POLARIZATION

### 2.1. Circular Polarization of the LCX

The structure of a leaky coaxial cable is similar to that of a coaxial cable but different in the outer conductor. Fig. 1 illustrates the common configuration of an LCX, whose aperture is symmetrical along the $z$-axial. The aperture is equivalent to a magnetic dipole, and the displacement current crossing the aperture generates an electric field along the LCX [9]. Therefore, the electric field is mainly the linear polarization in the maximum gain direction. On the contrary, the electric field component $E_\varphi$ exists when the aperture is not symmetrical along $z$-axial as shown in Fig. 2 for reference. Such a shape of the LCX will show an elliptic polarization characteristic, and the accuracy polarization characteristic is determined by the magnitude and the phase of the $E_\varphi$ and $E_z$. Due to the exponential decay of $E_r$ with increasing radial distance from the LCX, it is only necessary to consider $E_\varphi$ and $E_z$ in general, where $E_r$ presents the near-field component in the radial direction. By choosing appropriate aperture, it is possible to have a better circular polarization characteristic.

Circular polarization characteristic is usually presented by the axial ratio ($AR$), which is defined

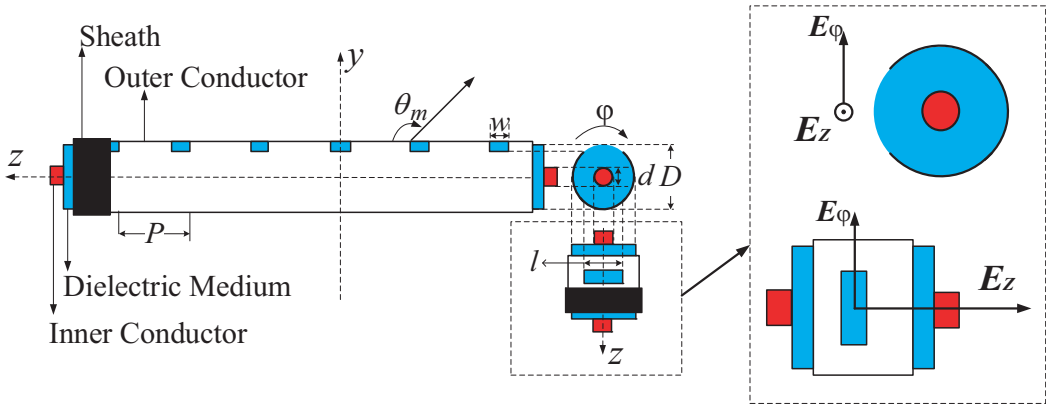


**Figure 1.** Common configuration of leaky coaxial cable (I-shape) and electric field.

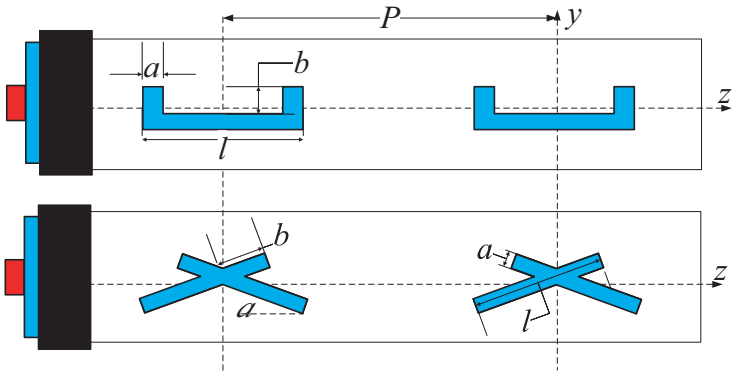


**Figure 2.** The U-shape LCX and the X-shape leaky coaxial cable with the proposed method.

as:

$$AR = \frac{E_{\max}}{E_{\min}} \tag{1}$$

where $E_{\max}$ and $E_{\min}$ are the maximum and minimum values of the instantaneous electric field, and they are also the long and short axes of the polarized ellipse [10]. It is generally considered to be circular polarization when the axial ratio $AR < 3\,\text{dB}$. The magnitude of the electric field is presented as follows:

$$E = \frac{\sqrt{2}E_\phi E_z \sin\delta}{\sqrt{E_\phi^2 + E_z^2 + \sqrt{(E_\phi^2 - E_z^2)^2 + 2E_\phi^2 E_z^2 \cos^2\delta}}} \tag{2}$$

where $\delta$ is the phase difference of $E_z$ and $E_\varphi$, and $E_{\max}$ and $E_{\min}$ are calculated by Eq. (2). $E_z$ and $E_\varphi$ satisfy the two conditions below:

(1) Amplitudes of $E_z$ and $E_\varphi$ are approximately equal to each other.
(2) The phase difference of $E_z$ and $E_\varphi$ is $\delta = \pi * k + \pi/2$, $k \in Z$.

### 2.2. Electrical Performances and Radiation Characteristics

It also needs to satisfy the electrical performance requirements such as the radiation mode, radiation direction, polarization gain and coupling loss in the working frequency band. In this case, the LCX needs to work in the condition of the single-mode radiation [11], then the circular polarization should exist in the maximum radiation direction, and the coupling loss must also meet the requirements of communication quality. Coupling loss is particularly suitable for evaluating the performance of the LCX's radiation efficiency, which is defined as: $L_c = 10 \cdot \log_{10}^{(P_t/P_r)}$, where $P_r$ is defined as the received power of a standard dipole located 2 meters away from the LCX, and $P_t$ is the power transmitted in the LCX.

According to the Floquet theorem, the LCX is a kind of periodic structure, and the electric field distribution around the LCX can be written by

$$E(r,\phi,z) = E_p(r,\phi,z)e^{-j(\beta - j\alpha)z} \tag{3}$$

where $\alpha$ and $\beta$ are the attenuation constant and propagation constant, respectively. The Floquet theorem points out that there is no difference between the fields of each cycle period in an infinitely long periodic structure. Therefore, the field at a certain point and the field at another point in an adjacent cycle differ from a constant coefficient. The constant coefficient is generally a complex number. So $E_p$ in Eq. (3) is a periodic function of $z$, and $E_p$ can be expressed by Fourier series: $E_p = \sum_{m=-\infty}^{\infty} E_{pm}(r,\phi,z)e^{-j\frac{2m\pi}{p}z}$, so the $E(r,\phi,z)$ in Eq. (3) can be presented as:

$$E(r,\phi,z) = \sum_{m=-\infty}^{\infty} E_{pm}(r,\phi,z)e^{-j\frac{2m\pi}{p}z} \cdot e^{-j(\beta - j\alpha)z} = e^{-\alpha z} \sum_{m=-\infty}^{\infty} E_{pm}(r,\phi)e^{-j\left(\beta + \frac{2m\pi}{P}\right)z} \tag{4}$$

where $\beta = k_0\sqrt{\varepsilon_r}$, $P$ is the period between the same two apertures. The propagation for radiation from the $m$th harmonic in the radial direction needs to satisfy:

$$k_0^2 - \left(\beta + \frac{2m\pi}{P}\right)^2 = k_0^2 - \left(k_0\sqrt{\varepsilon_r} + \frac{2m\pi}{P}\right)^2 \geq 0 \tag{5}$$

where $k_0 = 2\pi f/c$. Therefore, the condition of radiation mode is obtained by Eq. (5).

$$-mf_1 < f < -mf_2 \quad (m = -1, -2, \ldots) \tag{6}$$

where $f_1 = \frac{c}{P\sqrt{\varepsilon_r}+1}$, $f_2 = \frac{c}{P(\sqrt{\varepsilon_r}-1)}$. Since usually the dielectric material of the LCX is made of the physical foam insulating medium (usually $1 < \varepsilon_r < 2$), $f_2 > 2f_1$, $(f_1, 2f_1)$ is the frequency range of the $-1$st radiation mode [12]. Considering $\cos\theta_m = (\beta + \frac{2m\pi}{P})/k_0$, $m$th radiation angle of the LCX is presented as follows:

$$\theta_m = \arccos\left(\sqrt{\varepsilon_r} + \frac{m\lambda}{P}\right) \tag{7}$$

## 3. DEMONSTRATION EXAMPLES OF CIRCULAR POLARIZATION FOR LCX

As shown in Fig. 2, the two new apertures are designed and analyzed according to the method mentioned above. Unlike the I-shape in Fig. 1, the U-shape LCX and X-shape LCX have the same aperture characteristics which are symmetrical about $y$-axis and asymmetrical about $z$-axis. $a$, $b$, $d$, $\alpha$ and $l$ are used to describe the shape of the apertures.

In order to ensure that the LCX is in the $-1$st radiation mode (single-mode radiation) at 900 MHz, the suitable pitch $P$ of the LCX needs to be calculated according to Eq. (5). The range of pitch is $P \in [P_{\text{Min}}, P_{\text{Max}}]$, where $P_{\text{Min}} = 157\,\text{mm}$, $P_{\text{Max}} = 314\,\text{mm}$. When the pitch $P < P_{\min}$, the LCX is in the surface wave mode [13]. $P_{\min} < P < P_{\text{Max}}$, and the LCX is in the $-1$st radiation mode with the radiation direction $\theta_{-1}$. The other high-order mode of the LCX appears, and there will be multiple radiation directions $\theta_m$ when $P > P_{\text{Max}}$. In this case, the electromagnetic power will be dispersed in multiple directions, which is not a rational use of the signal power. Therefore, it is necessary to make sure that it works in the $-1$st radiation mode.

For the common case, the transverse radiation pattern of the I-shape LCX is obtained as shown in Fig. 3(a). The pitch $P$ is 200 mm; the width $w$ is 6 mm; the diameter of the outer conductor $D$ is 43 mm; the diameter of inner conductor $d$ is 18 mm; the length of the LCX is $11 * P$ long; the characteristic impedance $R$ is 50 Ohms.

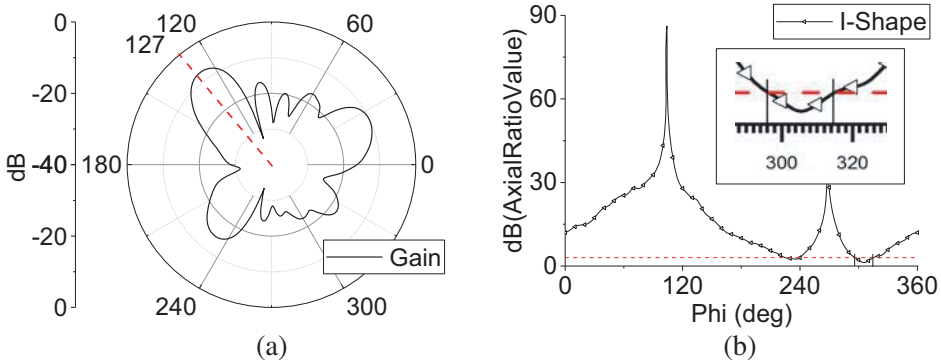


**Figure 3.** Radiation pattern and $AR$ of I-shape LCX. (a) Gain of the transverse radiation pattern ($f = 900\,\text{MHz}$). (b) Variation of Axis Ratio with $\varphi$.

As shown in Fig. 3(a), the direction of the maximum radiation can be located at $\theta = 127\,\text{deg}$, which is consistent with the theoretical calculation result $\theta_{-1} = 124.8\,\text{deg}$ according to Eq. (6) (relative dielectric constant $\varepsilon_r = 1.2$, pitch $P = 200\,\text{mm}$, velocity of light $c_0 = 3e8\,\text{m/s}$). The dashed red line indicates $AxialRatio = 3\,\text{dB}$ in Fig. 3(b), while there is only about 15 deg of the $AR$ that is less than 3 dB in the $\varphi$ range.

It can be seen that the radiation direction is only related to the pitch and dielectric material when the frequency is unchanged in Eq. (7). Therefore, the U-shape LCX and X-shape LCX have the same radiation direction as the I-shape LCX.

### 3.1. U-Shape LCX

The parameters $a$, $b$, and $l$ of the U-shape are swept at the maximum radiation direction. The $AR$ of the U-shape one is shown in Fig. 4.

It can be seen that the proposed U-shape LCX has the $\varphi$ ranges of $AR < 3\,\text{dB}$ under each combination of parameters. There is a range of $AR$ <3 dB when $\varphi \in [250\,\text{deg}, 310\,\text{deg}]$ in the maximum radiation direction ($a = 6\,\text{mm}$, $l = 80\,\text{mm}$, $b = 6\,\text{mm}$), which means that it has a circular polarization wave range of 60 deg with these parameters. Similarly, when $a = 6\,\text{mm}$, $l = 60\,\text{mm}$ and $b = 6\,\text{mm}$, the circular polarization wave range is $\varphi \in [200\,\text{deg}, 250\,\text{deg}]$ as shown in Fig. 4.

Figure 5 illustrates the variation of the U-shape LCX's gain with $\varphi$ where GainTotal is the gain calculated from the density of the electric field, and GainRHCP is the gain calculated from the electric

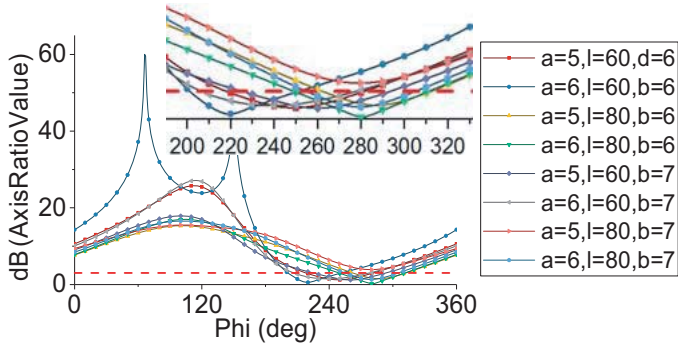


**Figure 4.** Variation of $AR$ with $\varphi$ of U-shape LCX ($a = 5\,\text{mm}/6\,\text{mm}$; $l = 60\,\text{mm}/80\,\text{mm}$; $b = 6\,\text{mm}/7\,\text{mm}$; $f = 900\,\text{MHz}$).

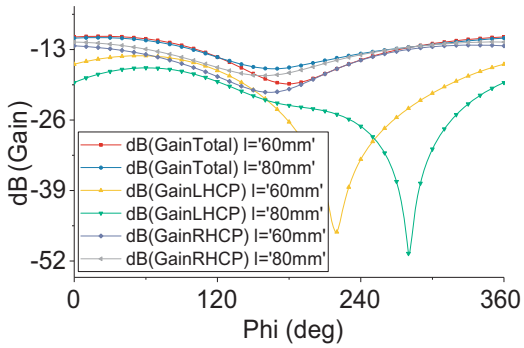


**Figure 5.** Variation of the gain with $\varphi$ of U-shape LCX ($a = 6\,\text{mm}$, $b = 6\,\text{mm}$, $l = 60\,\text{mm}/80\,\text{mm}$, $f = 900\,\text{MHz}$).

field density of the right-handed circular polarization. Similarly, GainLHCP represents the left-handed circular polarization gain. GainRHCP is the same as GainLHCP when it is linear polarization, while it is circular polarization when either gain is close to the GainTotal. It can be seen that the right-hand circular polarization gain approaches the total gain when $l = 60\,\text{mm}$ and $\varphi \in [200\,\text{deg}, 250\,\text{deg}]$, so the LCX radiates right-hand circular polarization wave. Similarly, it is right-hand circular polarization when $l = 80\,\text{mm}$ and $\varphi \in [250\,\text{deg}, 310\,\text{deg}]$.

### 3.2. X-Shape LCX

As shown in Fig. 6(a), the novel LCX with an X-shape aperture is simulated in the maximum radiation direction, which is under the conditions of pitch $P = 180\,\text{mm}/220\,\text{mm}$ and aperture length $l = 74\,\text{mm}/77\,\text{mm}/80\,\text{mm}$. That $\varphi \in [310\,\text{deg}, 350\,\text{deg}]$ and $\varphi \in [270\,\text{deg}, 300\,\text{deg}]$ are the ranges of circular polarization when pitches $P$ are 220 mm and 180 mm, respectively.

The curve of $l$ with $\varphi$ is mainly unchanged with the same value of pitch $P$. The tendency curve of $AR$ changes obviously when pitch $P$ changes. $AR$ curve has one sharp peak when $P = 180\,\text{mm}$, while the curve of $AR$ has two peaks when $P = 220\,\text{mm}$, which indicates that there is a very close relation between the $AR$ and the pitch. Selecting an appropriate pitch can expand the range of circular polarization wave.

As shown in Fig. 6(b) ($P = 220\,\text{mm}$, $l = 77\,\text{mm}$, $b = 10\,\text{mm}$), the results suggest that the total gain is almost the same as right-hand circular polarization gain in the area of $\varphi \in [270\,\text{deg}, 300\,\text{deg}]$, which means that the LCX radiates the right-hand circular polarization wave.

As seen in Table 1, for the I-shape LCX, there is only 15 degrees of the circular polarization range while the other two are at least 2 times that range of the I-shape LCX. Compared with the I-shape LCX, the new method design can indeed extend the circular polarization radiation range.

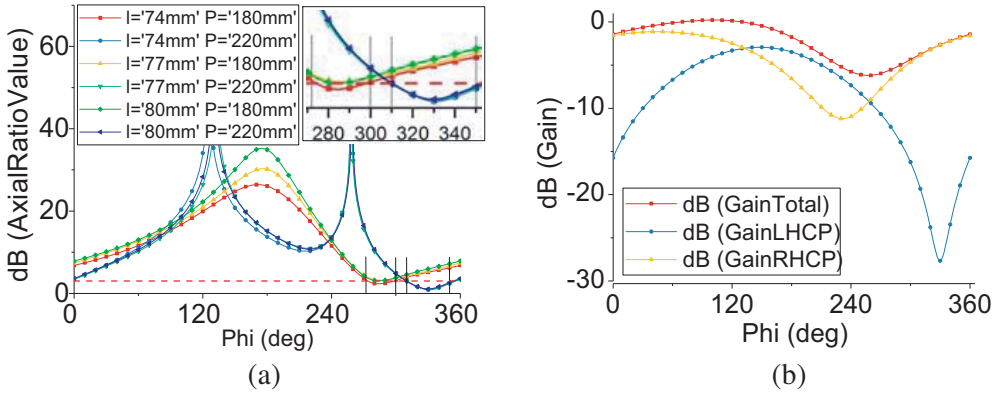


**Figure 6.** Characteristics of X-shape LCX. (a) Variation of axis ratio with $\varphi$ of x-shape LCX. (b) Gain characteristic of x-shape LCX.

### 3.3. Coupling Loss Testing

However, in practice, many sophisticated factors affect the performance of the LCX except circular polarization range. The range of circular polarization should cover the area of the mobile terminals, and it is also necessary to make sure that the coupling loss can meet the communication requirements. The coupling losses of those two novel LCXs are simulated in the same coupling test system as shown in Fig. 7(a). The simulation models are approximately optimized because of the complex structure of coupling loss test system. In the simulation model, the inner conductor of LCX is a cylinder made of copper, and the outer conductor is defined as PEC. The dielectric constant of the insulation medium is

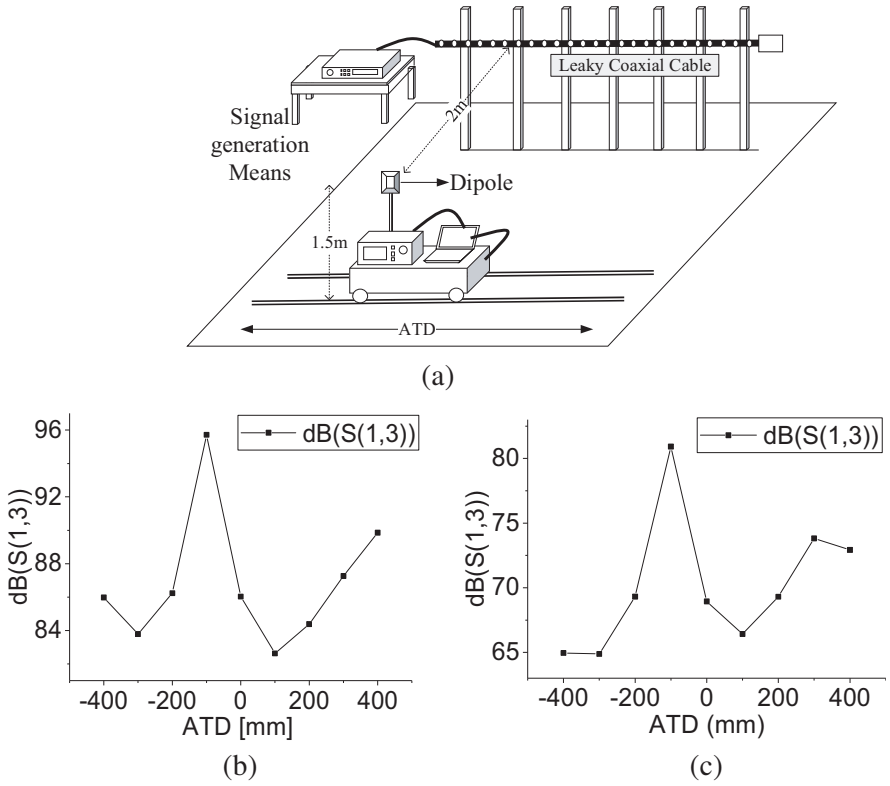


**Figure 7.** The simulation results of the coupling loss. (a) Coupling loss test system. (b) Coupling loss of the U-shape LCX. (c) Coupling loss of the X-shape LCX.

**Table 1.** Comparison of different type of LCX.

| **Type** | **I-shape** | **U-shape** | **X-shape** |
|---|---|---|---|
| **Range of *Coupling loss*** | 15 deg | $50 \sim 70$ deg | $30 \sim 40$ deg |

1.247, and dielectric loss angle tangent is 1.7e-5. The dipole antenna works at 900 MHz. Figs. 7(b)–7(c) illustrate the simulation results of coupling loss.

In Fig. 7, *ATD* presents the dipole antenna transformation distance. The coupling losses of the U-shape and X-shape LCXs are 84 dB and 67 dB, respectively. Larger absolute value of the coupling loss means less power radiated by the LCX and smaller power received by the dipole antenna. When coupling loss is great enough, it is difficult to meet communication requirements. In practical system requirements, the coupling loss of $85 \sim 105$ dB is generally specified as the greatest coupling loss that the communication system cannot use. Fortunately, the actual product performance is always better than the results of simulation model, and the difference between simulated and experimental results is $5 \sim 8$ dB, which confirms the good communication quality.

## 4. CONCLUSION

This paper introduces a method of LCX aperture designing in communication frequency band, which can realize the coverage of circular polarization wave within a certain range of the radiation angle. The results demonstrate that a wide circular polarization range can be achieved by optimizing the parameters of apertures. Circular polarization simulations are introduced to meet the requirements of the coupling loss index at 900 MHz. The study is significant in determining circular polarization wave and making improvement on designing aperture shape efficiently in theory. This new universal method is helpful for workers in the product installation, and it also provides guidance for the development of the novel LCX efficiently.

## REFERENCES

1. Wang, H., F. R. Yu, and H. Jiang, "Modelling of radio channels with leaky coaxial cable for LTE-M based CBTC systems," *IEEE Communications Letters*, Vol. 20, No. 5, 1038–1041, 2016.
2. Pan, Y. T., G. X. Zheng, and C. Oestges, "Characterization of polarized radio channel with leaky coaxial cable in a tunnel-like environment," *IEEE Antennas & Wireless Propagation Letters*, Vol. 16, 2803–2807, 2017.
3. Wu, Y. M., G. X. Zheng, and T. Wang, "Performance analysis of MIMO transmission scheme using single leaky coaxial cable," *IEEE Antennas & Wireless Propagation Letters*, Vol. 16, 298–301, 2017.
4. Harman, K. and W. K. Messner, "Outdoor perimeter security sensors a forty-year perspective," *IEEE International Carnahan Conference on Security Technology*, 1–9, IEEE, 2012.
5. Guan, Q., C. C. Chen, and C. X. He, "A novel sensor using VHF zigzag-slotted leaky coaxial cable for intruder localization," *Microwave and Optical Technology Letters*, Vol. 60, 634–639, 2018.
6. Mayama, K. and Y. Okano, "Development of nearby tags detection unit with UHF-RFID technology," *International Symposium on Antennas and Propagation*, IEEE, 2017.
7. Gao, G.-P., M. Li, S.-F. Niu, X.-J. Li, B.-N. Li, and J.-S. Zhang, "Study of a novel wideband circular slot antenna having frequency band-notched function," *Progress In Electromagnetics Research*, Vol. 96, 141–154, 2009.
8. Wang, J. H., "Leaky coaxial cable with circular polarization property," *IEEE Transaction on Antennas and Propagation*, Vol. 59, No. 2, 682–685, 2011.
9. Kim, S. T., G. H. Yun, and H. K. Park, "Numerical analysis of the propagation characteristics of multi-angle multi-slot coaxial cable using moment method," *IEEE Trans. on Microwave Theory and Technology*, Vol. 46, No. 3, 269–279, 1998.

10. Wang, L., X. Chen, and D. Wu, "A novel circular polarised antenna with wide power and axial-ratio beam width by using tilted dipoles," *Progress In Electromagnetics Research Letters*, Vol. 69, 37–43, 2017.
11. Wang, J. H. and K. K. Mei, "Design of leaky coaxial cables with periodic slots," *Radio Science*, Vol. 37, No. 5, 1–10, 2016.
12. Kim, S. T., G. H. Yun, and H. K. Park, "Numerical analysis of the propagation characteristics of multi-angle multi-slot coaxial cable using moment method," *IEEE Trans. on Microwave Theory and Technology*, Vol. 46, No. 3, 269–279, 1998.
13. Inomata, K., W. Tsujita, and T. Hirai, "Two-frequency surveillance technique for intrusion-detection sensor with Leaky Coaxial Cables," *Sensors Applications Symposium*, 103–106, IEEE, 2014.